16th World Conference on Earthquake Engineering, 16WCEE 2017
Santiago Chile, January 9th to 13th 2017
Paper N° 4789
Registration Code: S-O1464726469

Cloud analysis considering global dynamic instability

A. Miano[(1)], F. Jalayer[(2)], H. Ebrahimian[(3)], A.Prota[(4)], G. Manfredi[(5)]

[(1)] PhD Candidate, Dept. of Structures for Engineering and Architecture, University of Naples "Federico II", andrea.miano@unina.it
[(2)] Associate Prof., Dept. of Structures for Engineering and Architecture, University of Naples "Federico II", fatemeh.jalayer@unina.it
[(3)] Post-doc Res., Dept. of Structures for Engineering and Architecture, University of Naples "Federico II", ebrahimian.hossein@unina.it
[(4)] Full Prof., Dept. of Structures for Engineering and Architecture, University of Naples "Federico II", a.prota@unina.it
[(5)] Full Prof., Dept. of Structures for Engineering and Architecture, University of Naples "Federico II", gaetano.manfredi@unina.it

Abstract

Cloud Analysis is based on simple regression in the logarithmic space of structural response versus seismic intensity for a set of registered records. This method is particularly efficient since it involves non-linear analysis of the structure subjected to a set of un-scaled ground motion time-histories. The simplicity of its underlying formulation makes it a quick and efficient analysis procedure for fragility assessment and/or performance-based safety-checking. Nevertheless, the Cloud Analysis has some limitations; such as, the assumption of a constant conditional standard deviation for probability distribution of the structural response given intensity. Arguably, with the increasing levels of intensity, the conditional dispersion in displacement-based response parameters given intensity may increase. Another complication arises when the structure becomes dynamically unstable (or when the analysis software encounters non-convergence problems, or the Collapse of the building due to large demands takes place) by subjecting to some of the ground motion records used for Cloud Analysis. In such cases, the assumption that structural response given intensity is described by a Log Normal probability distribution with constant standard deviation (one of the underlying assumptions of the Cloud Analysis) no longer holds. However, the method can still be applied to the portion of Cloud response that does not include cases of dynamic instability. Thus, the probability of exceeding a specific structural response value given ground motion intensity can be expressed, using the Total Probability Theorem, as the sum of two probability terms. These terms correspond to the two mutually exclusive and collectively exhaustive portions of the Cloud response; namely, without cases of dynamic instability and with cases of dynamic instability. In such formulation, the probability of dynamic instability given seismic intensity can be calculated by using a generalized regression model (e.g., logistic regression). The transverse frame of a seven-story existing building in Van Nuys, CA, which is modeled in OpenSees considering the flexural-shear-axial interactions, is employed in order to demonstrate this procedure. The critical demand to capacity ratio, corresponding to the component or mechanism that leads the structure closest to the onset of limit state (e.g., near collapse), is adopted as the structural response parameter. This structural response parameter, that is equal to unity at the onset of limit state, can encompass both ductile and fragile failure mechanisms. Moreover, it can register a possible shift in the governing failure mechanism with increasing intensity. The results for probabilistic demand assessment based on the Cloud Analysis considering the cases of dynamic instability are compared with those obtained based on non-linear dynamic analysis methods such as Incremental Dynamic Analysis and Multiple Stripe Analysis. It is demonstrated that, with a careful selection of ground motion records, this method leads to reasonably accurate results with considerably reduced analysis effort.

Keywords: Cloud Analysis; Non-linear Dynamic Analysis methods; Generalized Regression Model; Performance-based Seismic Assessment; Probability of Collapse

1. Introduction

Many existing reinforced concrete (RC) moment-resisting frame buildings in regions with high seismicity were built without adequate seismic-detailing requirements and are particularly collapse-prone buildings. Identifying accurately the level of performance can facilitate an efficient seismic assessment and classification of these buildings. In this context, analytic structural fragility assessment is one of the fundamental steps in the modern performance-based engineering [1]. The structural fragility can be defined as the conditional probability of exceeding a prescribed limit state given the intensity measure (IM). There are alternative non-linear dynamic analysis procedures available in the literature for characterizing the relationship between engineering demand parameters (EDPs) and IM based on recorded ground motions, such as, the Incremental Dynamic Analysis (IDA, [2] Multiple-Stripe Analysis (MSA, see [3]) and the Cloud Method [4-10]. The nonlinear dynamic methods such as IDA and MSA are suitable for evaluating the relationship between EDP and IM for a wide range of IM values; however, their application can be quite time-consuming as the non-linear dynamic analyses are going to be repeated (usually for scaled ground motions) for increasing levels of IM.

The Cloud Method is particularly efficient since it involves the non-linear analysis of the structure subjected to a set of un-scaled ground motions. The simplicity of its underlying formulation makes it a quick and efficient analysis procedure for fragility assessment [7-10] or safety-checking [6]. Nevertheless, the Cloud Analysis has two main limitations: (a) it is assumed that the conditional standard deviation in EDP given IM is a constant and does not depend on the intensity level, (b) complication arises when the structure experiences global dynamic instability (manifesting itself as very high global displacement-based demands or non-convergence problems in the analysis software) due to a certain record or records belonging to the suite of records used for Cloud Analysis. In the latter, the assumption of describing the EDP given IM as a Log Normal probability distribution with constant standard deviation (one of the underlying assumptions of the Cloud Analysis) no longer holds. However, the method can still be applied to the portion of Cloud response that does not include cases of dynamic instability. Thus, the probability of exceeding a specific level of EDP given IM can be expressed as the sum of two mutually exclusive and collectively exhaustive terms using the Total Probability Theorem [11], addressing the portion of the Cloud response without cases of dynamic instability and with cases of dynamic instability, respectively. Accordingly, the probability of global dynamic instability given IM can be calculated by using a generalized regression model (herein, logistic regression).

As a numerical example, the transverse frame of a seven-story existing RC building in Van Nuys, CA, modeled in Opensees by considering the flexural-shear-axial interactions in the columns, is employed. Because of the old construction philosophy, column members are sensible to possible shear failure during earthquakes; hence, a non-linear model is used to predict an envelope of the cyclic shear response [12, 13]. This envelope includes the shear displacement and corresponding strength predictions at the peak strength, onset of lateral strength degradation, and loss of axial-load-carrying capacity. The adopted engineering demand parameter (EDP) is the critical demand to capacity ratio [14] corresponding to the component or mechanism that leads the structure closest to the onset of near collapse limit state. This structural response parameter, that is equal to unity at the onset of the desired limit state, can encompass both ductile and fragile failure mechanisms. The results for probabilistic demand assessment based on the Cloud Analysis with explicit consideration of the cases of global dynamic instability, are compared with those obtained based on IDA. It is demonstrated that, with a careful selection of ground motion records, this method leads to reasonably accurate results with considerably reduced analysis effort.

2. Methodology

2.1. Structural Performance Variable

The EDP herein is taken to be the critical demand to capacity ratio [10, 14] denoted as Y_{LS} and defined as the demand to capacity ratio for the component or mechanism that brings the system closer to the onset of limit state *LS* (herein, the near collapse limit state). The formulation is based on the cut-set concept [15], which is suitable

for cases where various potential failure mechanisms (both ductile and fragile) can be defined a priori. Y_{LS} , which is always equal to unity at the onset of limit state, is defined as:

$$Y_{LS} = \max_{l}^{N_{mech}} \min_{j}^{N_l} \frac{D_{jl}}{C_{jl}(LS)} \quad (1)$$

where N_{mech} is the number of considered potential failure mechanisms; N_l the number of components taking part in the lth mechanism; D_{jl} is the demand evaluated for the jth component of the lth mechanism; $C_{jl}(LS)$ is the limit state capacity for the jth component of the lth mechansim. The capacity values refer to the near collapse limit state in this work, but the procedure can be repeated for any other prescribed limit state. In the context of this work, D is the demand expressed in terms of maximum chord rotation for the component, denoted as θ_{max}, and computed based on the nonlinear dynamic analysis. C is the component chord rotation capacity denoted as $\theta_{ultimate}$, $\theta_{yielding\text{-}flexure}$, or θ_{axial} corresponding to the ultimate, flexural yield, and axial capacities, respectively:

- $\theta_{ultimate}$ corresponds to the point on the softening branch of the force-deformation curve of the member (taking into account the nonlinear deformations associated with flexure and shear), where a 20% reduction in the maximum strength takes place
- $\theta_{yielding\text{-}flexure}$ corresponds to the point where the yielding of the reinforcements takes place in the flexural force-deformation relationship of the member.
- θ_{axial} corresponds to the point associated with the complete loss of vertical-load carrying capacity of the component on the softening branch.

In summary, the possible failure mechanisms in this study can be categorized as:

Table 1 – Potential failure mechanisms

Failure Type	**Component(s)**	**Definition / Description**
Ductile	column / beam	$\theta_{max}>\theta_{ultimate}$
Brittle	column	
Soft-story mechanism	all columns of one story	$\theta_{max}>\theta_{yielding\text{-}flexure}$
Partial mechanism	for a number of adjacent stories: all beams + bottom and top columns	$\theta_{max}>\theta_{yielding\text{-}flexure}$
Global mechanism	for the entire building: all beams + base columns	$\theta_{max}>\theta_{yielding\text{-}flexure}$

*Note that θ_{max} refers to the flexural portion of component chord rotation when compared to $\theta_{yielding\text{-}flexure}$

When predicting non-linear response of structures, it is necessary to account for the possibility that some records may cause global "*Collapse*"; i.e., very high global displacement-based demands or non-convergence problems in the analysis software. It is obvious that, $Y_{LS}>1$ for the limit state of near-collapse does not guarantee the exceedance of collapse limit state. Herein, the cases of collapse are identified explicitly by verifying the following criteria for structural collapse:

Table 2 – Potential global "*Collapse*" mechanisms

Collapse Type	**Component(s)**	**Definition / Description**
Ductile	50% +1 of the columns of one story (adopted somehow arbitrarily herein)	$\theta_{max}>\theta_{ultimate}$
Brittle	50% +1 of the columns of one story (see [16])	$\theta_{max}>\theta_{axial}$

2.2. Nonlinear Dynamic Analysis Procedure

In order to estimate the structural fragility, Cloud Analysis is adopted herein as the nonlinear dynamic analysis procedure. For a suite of ground motion waveforms, the cloud data encompass pairs of ground motion IM and its corresponding structural performance variable Y_{LS} (see Eq. 1) for each record. Herein, IM is adopted as the spectral acceleration at the first-mode period, $Sa(T)$. The cloud data can be separated to two parts: (a) NoC data

which correspond to that portion of the suite of records for which the structure does not experience "*Collapse*", (b) *C* data for which the structure leads to "Collapse" (see Table 2). The fragility, expressed generally as the conditional distribution of Y_{LS} given *Sa*, can be expanded with respect to *NoC* and *C* data as follow using the Total Probability Theorem (see also [3, 7]):

$$P\left(Y_{LS}>1|\,Sa\right)=P\left(Y_{LS}>1|\,Sa,NoC\right)\times P\left(NoC\,|\,Sa\right)+P\left(Y_{LS}>1|\,Sa,C\right)\times P\left(C\,|\,Sa\right) \quad (2)$$

The probability terms in Eq. (2) are described clearly as follows:

- The *NoC* term $P(Y_{LS}>1|Sa,NoC)$ is the conditional distribution of $Y_{LS}|Sa$ given *NoC*, and can be described by a lognormal distribution (a widely used assumption that has been usually verified for cases where the regression residuals represent unimodal behaviour, see e.g. [3, 5]):

$$P\left(Y_{LS}>1|\,Sa,NoC\right)=P\left(\ln Y_{LS}>0\,|\,Sa,NoC\right)=1-\Phi\left(\frac{-\ln\eta_{Y_{LS}|Sa,NoC}}{\beta_{Y_{LS}|Sa,NoC}}\right)=\Phi\left(\frac{\ln\eta_{Y_{LS}|Sa,NoC}}{\beta_{Y_{LS}|Sa,NoC}}\right) \quad (3)$$

where Φ is the standardized Gaussian cumulative distribution function (CDF), $\eta_{YLS|Sa,NoC}$ and $\beta_{YLS|Sa,NoC}$ are conditional median and standard deviation (dispersion) of the natural logarithm of Y_{LS} for *NoC* data. Based on the standard Cloud Analysis procedure, these two parameters can be directly obtained by performing a logarithmic linear regression on the *NoC* data. Assuming N_{NoC} be the number of *NoC* data:

$$\ln\eta_{Y_{LS}|\,Sa,NoC}=\ln a+b\ln\left(Sa\right),\ \ \beta_{Y_{LS}|\,Sa,NoC}=\sqrt{\frac{\sum_{\Omega_{NoC}}\left(\ln Y_{LS}-\ln a-b\ln(Sa)\right)^2}{N_{NoC}-2}} \quad (4)$$

- The *C* term $P(Y_{LS}>1|Sa,C)$ is the conditional distribution of $Y_{LS}|Sa$ given *C* and is equal to unity, i.e. in the cases of global dynamic instability (global Collapse), the limit state *LS* is certainly exceeded.
- The term $P(C|Sa)=1-P(NoC|Sa)$ is probability of global dynamic instability (Collapse), which can be expressed by a logistic regression model (a.k.a., logit) on the *Sa* values of the entire cloud data:

$$P\left(C\,|\,Sa\right)=\frac{1}{1+e^{-\left(\beta_0+\beta_1.Sa\right)}} \quad (5)$$

where β_0 and β_1 are the parameters of the logistic regression. It is to note that the logistic regression model belongs to the family of generalized regression models and is particularly useful for cases in which the regression dependent variable is binary (i.e., can have only two values 1 and 0, *yes* or *no*, which is the case of *C* and *NoC* herein). Note that the logistic regression model described above is applied to all records; they are going to be distinguished by 1 or 0 depending on whether they lead to *C* or *NoC*.

3. Numerical Application

3.1. Building Model Description

The transverse frame of the seven-story existing Van Nuys Hotel building in the San Fernando Valley of Los Angeles County, CA [3, 7, 8 17] is re-modeled using OpenSees (http://opensees.berkeley.edu, ver. 2.4.5), considering the flexural-shear-axial interactions (see Fig. 1a). The structure was originally designed in 1965 according to the 1964 Los Angeles City Building Code, and built in 1966. The building was severely damaged in the M 6.7 1994 Northridge earthquake. After the 1994 earthquake, the building was retrofitted with new reinforced concrete shear walls; however, the modeling features are consistent with the original building prior to the 1994 Northridge earthquake. The structural system is cast-in-place RC moment-resisting frame, regular in elevation, with non-ductile column detailing according to the new Building Regulations. Lateral force resistance is provided primarily by the perimeter moment frames, although the interior columns and flat slabs also

contribute to lateral stiffness. The information regarding section dimensions, reinforcement bars, ties, and material properties for all the frame elements are summarized in [17].

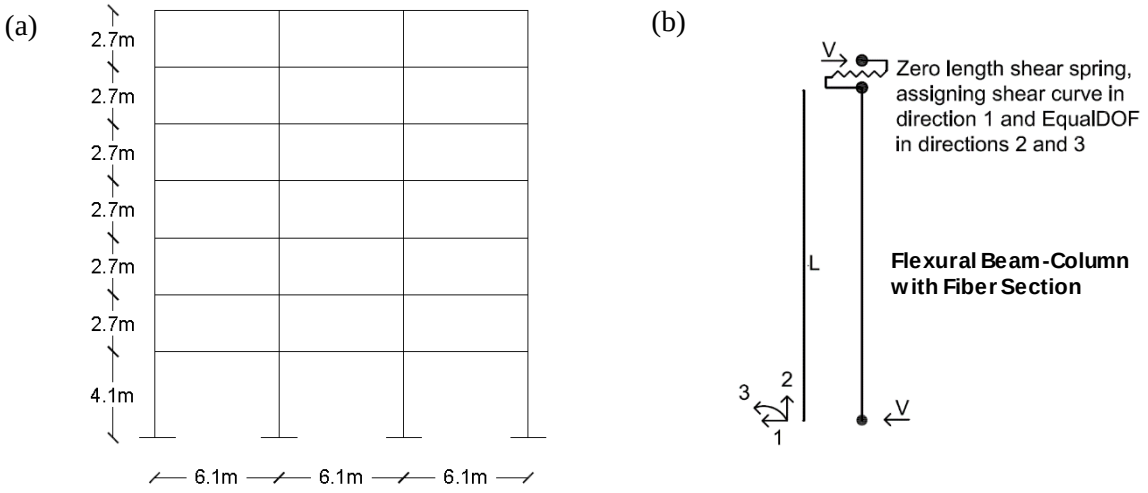

Fig. 1 – (a) Geometric configuration of the transverse frame, (b) Elements used for modeling the columns in the Combined Model

Two different models of the existing frame is developed herein: (a) *Flexural Model* considers only the flexural-axial behavior of the beam-column members; (b) *Combined Model* takes into account the flexural-shear-axial interactions of the columns, assuming a total lateral deformation response as the sum of two different contributions (i.e., flexure and shear). Although modeling issues are not the primary goal of this paper, they are, however, key features in the assessment of an existing building; thus, they should be verified carefully. The beams and columns are modeled using force-based beam-column elements considering fiber-sections in OpenSees. Plastic hinge integration method (herein, Modified Radau Hinge Integration, [18]) is used to assign inelastic actions at the end regions of the element with specified length while the remainder of the element behaves linearly elastic. Concrete behavior is simulated using the Concrete01 material with peak strength achieved at a strain of 0.002 and minimum post-peak strength achieved at a strain of 0.004. Longitudinal reinforcing steel is modeled using the Steel02 material with a post-yield modulus equal to 1% of the elastic modulus. Each RC column in the Combined Model is defined using the flexural beam-column and the shear spring elements in series, as shown schematically in Fig. 1b. Thus, the total displacement response is the sum of the displacement of each element.

The shear springs are implemented in OpenSees as a zero-length element with a uniaxial hysteretic material and the force-deformation following the shear curve in the direction of shear force. For modeling the nonlinear shear behavior of columns, the lateral force/shear displacement curve of the columns are estimated with three points (see [12]: (a) maximum shear strength and corresponding shear displacement; (b) onset of shear strength degradation; (c) shear displacement at axial load failure. The shear strength is calculated using the model proposed by [19], which has a factor k to account for ductility-related strength degradation:

$$V_n = V_s + V_c = k\frac{A_v\, f_y\, d}{s} + k\left(\frac{0.5\sqrt{f_c}}{a/d}\sqrt{1+\frac{P}{0.5\sqrt{f_c}\,A_g}}\right)0.8\,A_g \tag{6}$$

where V_s and V_c are the contributions of stirrups and concrete to shear strength; A_v is the transverse reinforcement area with a spacing s in the loading direction; f_y is the transverse reinforcement yield strength; d is the section depth; f_c is the compressive strength of concrete; a is the shear span of the element; P is the axial load of the section; A_g is the gross area of the section; k equals 1.0 for displacement ductility less than 2, to be equal to 0.7 for displacement ductility exceeding 6, and to vary linearly for intermediate displacement ductilities. The total response of the column due to shear and flexure is obtained herein by on pre-analysis column failure

category classification according to [12]. This task is accomplished by comparing the shear strength V_n, the yield strength V_y, and the flexural strength Vp of columns. The displacement at the onset of shear failure, $\Delta_{v,u}$, is adopted from [20], and is calculated as:

$$\Delta_{v,u} = (4 - 12 \cdot \frac{v_n}{fc}) \cdot \Delta_{v,n} \tag{7}$$

where v_n is the shear stress at peak strength ($v_n=V_n/bd$, where b is the column width); $\Delta_{v,n}$ is the shear displacement at peak strength computed by Response-2000 (http://www.ecf.utoronto.ca/~bentz/home.shtml, [21]). The shear displacement at axial load failure, $\Delta_{v,f}$, is calculated as:

$$\Delta_{v,f} = \Delta_{ALF} - \Delta_{f,f} \geq \Delta_{v,u} \tag{8}$$

where Δ_{ALF} is the total displacement at axial load failure and $\Delta_{f,f}$ is the flexural displacement at the point of axial load failure. It is noteworthy that the bar slip contribution to the total displacement of the element has been neglected herein. The total displacement at axial load failure is defined as follows [22]:

$$\Delta_{ALF} = \frac{4}{100} \frac{1 + \tan^2 \theta}{\tan \theta + P\left(\frac{s}{A_v f_y d_c \tan \theta}\right)} \cdot L \tag{9}$$

where tan θ is the angle of shear crack, and d_c is the depth of the concrete core. Fig. 2 illustrates the flexural, shear, and the combined force-deformation curves for central column in the second story for the Combined Model. The three above-mentioned points are demonstrated on the component shear lateral force-deformation diagram (Fig2.b): point 1 is the maximum strength point V_n, point 2 shows the onset of shear degradation $\Delta_{v,u}$, and finally point 3 is the axial load failure $\Delta_{v,f}$. With reference to the flexural curve, $\theta_{\text{yielding-flexure}}$ corresponds to the demand associated with the cyan dot point (Fig2.a). In addition, θ_{ultimate} is defined with red star on the total lateral force-displacement curve (Fig2.c) while the red dot point shows θ_{axial} correspond to the axial failure.

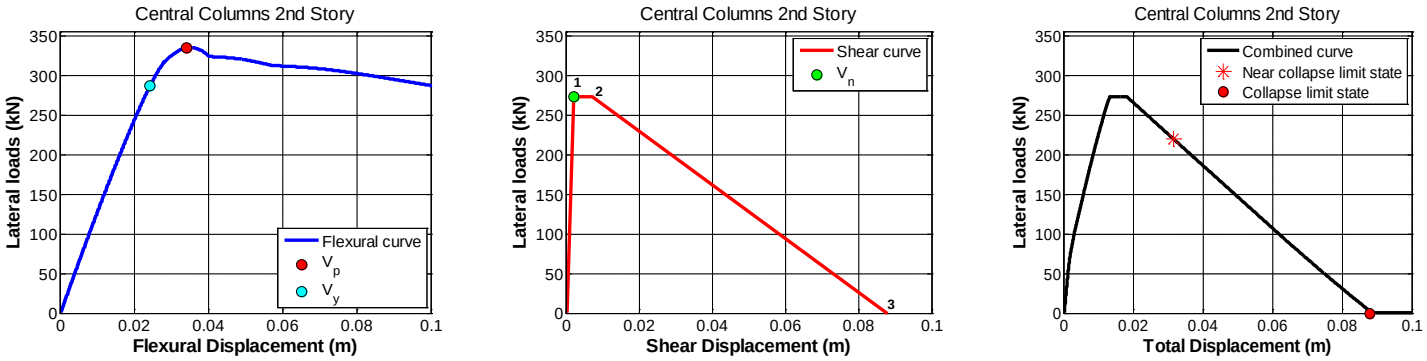

Fig. 2 – The flexural, shear, and the total force-deformation curves, the Combined Model

3.2. Ground-Motion Selection

A set of 35 ground motion records are used based on the Silva Catalog [7, 22] for different sites in California. These records were all recorded on stiff soil (Geo-Matrix soils types C and D, V_s^{30}=259÷569 m/s) and were selected from a moment magnitude in the range of 5.0<M<7.5 and "Joyner-Boore" site-to-source-distance (defined as the shortest distance from a site to the surface projection of the rupture plane) in the range of 0.1km<R<115km. It is to note that two specific criteria have been used for records selection: (1) making sure that the suite of selected records achieve high a high dispersion in the adopted intensity measure (herein, first-mode spectral acceleration); (2) making sure that the suite of selected records manages to cover both sides of Y_{LS}=1 in a roughly balanced manner (in simple terms: making sure that several records lead to Y_{LS}>=1).

The nonlinear dynamic analysis methods, presented in the next section, are based on this sample of 35 records. Fig. 3 illustrates the spectral acceleration of the suite of 35 records. Note that the spectral acceleration at the first-mode period, $Sa(T_1)$, is the IM used in this study where T_1 is 0.78 sec and 0.89 sec for the Flexural and Combined Models, respectively.

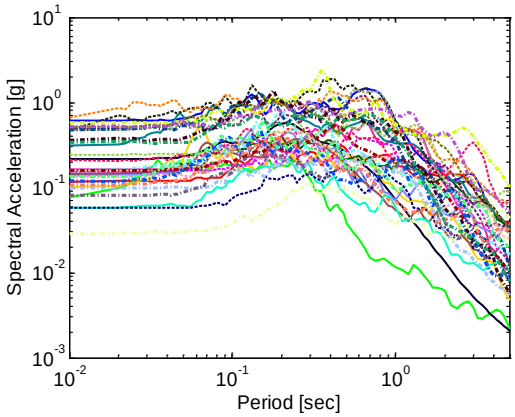

Fig. 3 – The spectral acceleration of the suite of 35 records used in this study

3.3. Cloud analysis

As explained comprehensively in Section 2.2, the Cloud Analysis is a nonlinear dynamic procedure in which the structure is subjected to a set of (un-scaled) ground motion records covering a wide range of IM, herein $Sa(T_1)$, values. The generated cloud data are the pairs of $[Y_{LS}, Sa]$ associated with the suite of ground motion waveforms. The "Cloud" method provides estimates of the two statistical parameters of $Y_{LS}|Sa$, namely the median and standard deviation, by performing a logarithmic linear regression on the cloud data. Accordingly, in cases where the "Collapse" or the global dynamic instability of the structure do not take place due to records in the suit of ground motions, (i.e., no *C* data exist), the fragility expressed as $P(Y_{LS}>1|Sa)$ can directly be estimated from Eq. (3) based on the logarithmic linear regression on the entire cloud data. On the other hand, if *C* data exist (there are records that cause Collapse), the fragility is calculated directly by implementing Eq. (2) using the logarithmic linear regression on the *NoC* data (Eq. 4), and a logistic regression on the entire cloud data (Eq. 5).

Fig. 5a shows the Cloud data and the associated Cloud regression for the flexural model where no *C* data exist. For each scatter Cloud response (colored squares), the corresponding record ID is shown. Accordingly, Fig. 5b illustrates the same results for the Combined Model, where 2 records out of 35 ground motions cause global dynamic instability (*C* data) as shown with red-colored squares. The estimated median and dispersion are shown on the figures separately. Moreover, the line $Y_{LS}=1$ corresponding to the onset of Near Collapse limit state is shown with red-dotted line on each figure. The lognormal distribution shown in Fig. 5a denotes the distribution of Y_{LS} given that $Sa(T_1)=0.15$g, while the lognormal distribution shown in Fig. 5b indicates the distribution of $Y_{LS}|Sa(T_1)=0.20$g.

In addition, the fragility curves for both models are calculated; for the Combined Model with collapse-cases, the expression in Eq. (2) considering the collapse-cases explicitly by a Logistic regression model is plotted as thick black lines. This curve is compared with the fragility curves calculated from Eq. (3) considering only the non-collapse data (dashed grey line). It can be seen that the explicit consideration of collapse-cases based on the procedure described in Section 2.2 leads to a slight difference (the fragility shifts to the left which means that the structure becomes slightly more vulnerable).

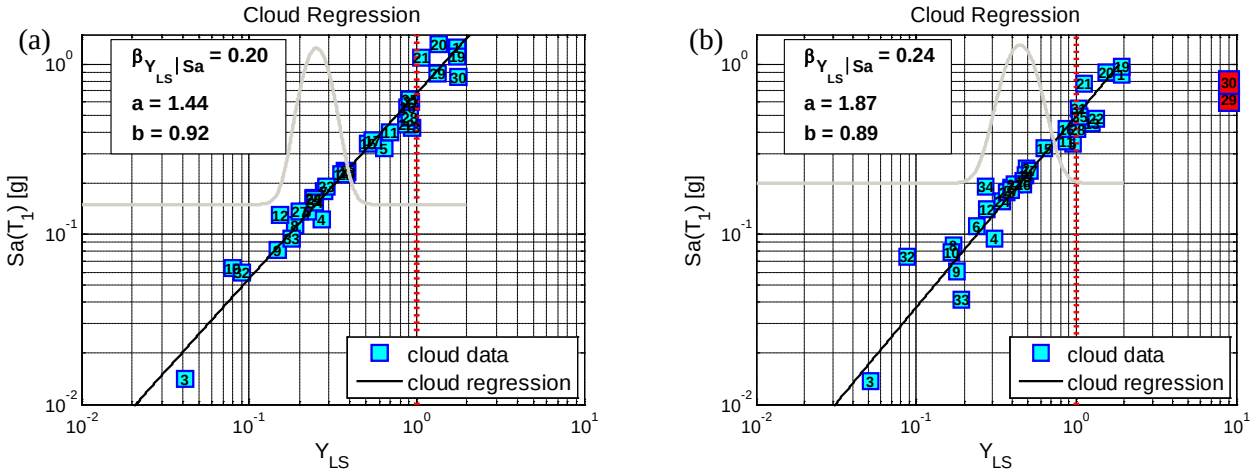

Fig. 4 – The Cloud Regression for (a) Flexural Model, (b) Combined Model

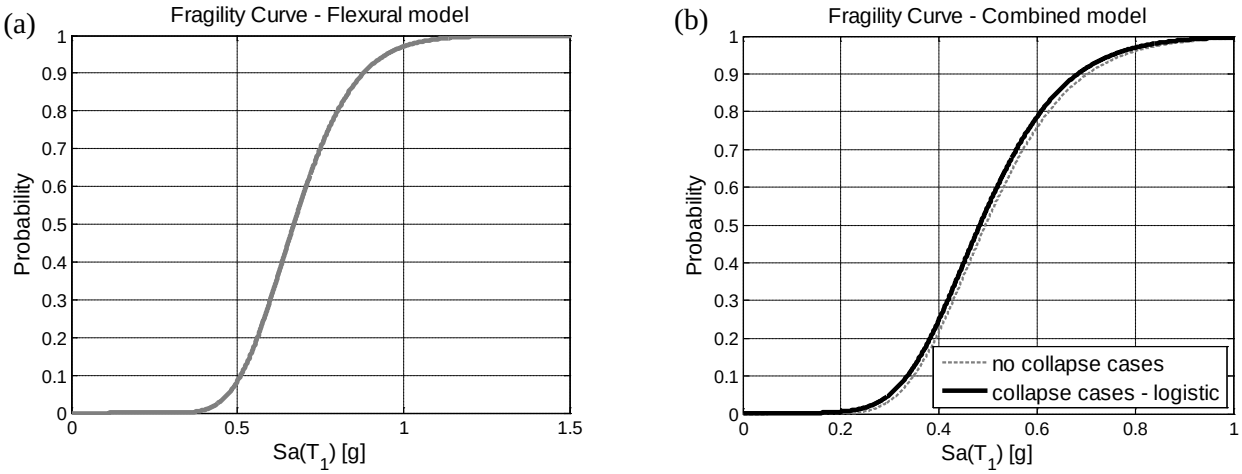

Fig. 5 – The fragility curves for the Near Collapse limit state (a) Flexural Model, (b) Combined Model

The fragility function as expressed in Eq. (2) is actually a Complementary CDF (CCDF) for the exceedance of Near Collapse limit state where Y_{LS}>1. Accordingly, the CDF of $Y_{LS}|Sa$ for a given demand y_{LS} can be denoted as $F_{YLS|Sa}(y_{LS})$, and derived as follows [7]:

$$F_{Y_{LS}|Sa}\left(y_{LS}\right) = P\left(Y_{LS} \le y_{LS} \mid Sa\right) = \left[1 - P\left(Y_{LS} > y_{LS} \mid Sa, NoC\right)\right] P\left(NoC \mid Sa\right)$$
$$= P\left(Y_{LS} \le y_{LS} \mid Sa, NoC\right) P\left(NoC \mid Sa\right) = \Phi\left(\frac{\ln y_{LS} - \ln \eta_{Y_{LS}|Sa,NoC}}{\beta_{Y_{LS}|Sa,NoC}}\right) P\left(NoC \mid Sa\right) \quad (10)$$

Eq. (10) can be used in order to calculate the demand value, y^p_{LS}, corresponding to percentile p of the distribution $F_{YLS|Sa}$ (i.e., the p% demand value) by setting the left side of the equation equal to p and solving it for y^p_{LS}:

$$y^p_{LS} = \eta_{Y_{LS}|Sa,NoC} \cdot \exp\left(\beta_{Y_{LS}|Sa,NoC} \cdot \Phi^{-1}\left(\frac{p}{P\left(NoC \mid Sa\right)}\right)\right) \quad (11)$$

where Φ^{-1} is the inverse function of standardized normal distribution. Fig. 6 shows the 16th, 50th and 84th percentiles of the demand response Y_{LS} as a function of the spectral acceleration for the Combined model in two different cases: (a) considering only *NoC* data where $P(NoC|Sa)$ becomes 1 in Eq. (11); (b) taking into account Collapse information (*C* data) where $P(NoC|Sa)$ is estimated based on the Logistic Regression model (Eq. 5) for different spectral acceleration levels. It is revealed that the percentiles in the two cases are very close up to Y_{LS}=1. The deviation of the predictions, as can be anticipated, are associated with large demand values Y_{LS}>1. As

a result, calculation of percentiles by using Eq. (11) considering the Collapse information has the advantage of "catching" the flattening of percentile curves associated with the occurrence of global Collapse of the structure at high demand values.

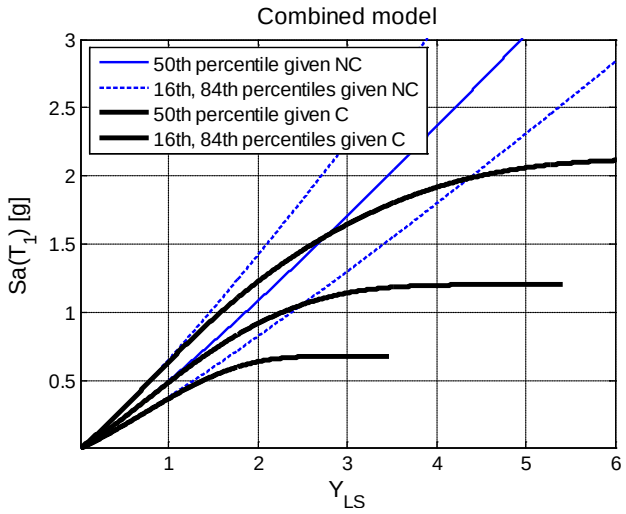

Fig. 6 – The 16th, 50th and 84th percentiles of performance variable Y_{LS} given Sa estimated based on the Cloud analysis using only no-collapse data, and also considering Collapse data

3.4. IDA analysis

Each IDA curve herein shows the variation in the performance variable Y_{LS} for a given ground motion record as a function of $Sa(T_1)$ while the record is scaled-up linearly in amplitude. Fig. 7 illustrates the IDA curves (in thin grey lines) with respect to Y_{LS} for the suite of 35 ground-motions defined in Section 3.2, considering both Flexural and Combined Models. The vertical red line plotted at Y_{LS}=1 demonstrates the dispersion in the spectral acceleration values $Sa_{Y=1}$ plotted as red-star points. The figure also demonstrates the (Log-Normal) probability density function fitted to the $Sa_{Y=1}$ values. This probability density is later represented in the form of a CDF to define the fragility function associated with IDA results (see also [14]). The horizontal red-dashed line represents the median of $Sa_{Y=1}$ values (denoted as $\eta_{SaY=1}$) from IDA analysis. In order to facilitate the comparison with Cloud Analysis results, the corresponding Cloud data (the squares) and the regression prediction (blue line) are also plotted. The spectral acceleration value corresponding to Y_{LS}=1 from the Cloud regression prediction (derived as $\eta_{SaY=1,Cloud} = (1/a)^{1/b}$) represents the median spectral acceleration capacity corresponding to Cloud analysis for the Near Collapse limit state. The horizontal blue dash-dotted line represents $\eta_{SaY=1,Cloud}$, which can be compared with the $\eta_{SaY=1}$ from the IDA results.

(a) (b)

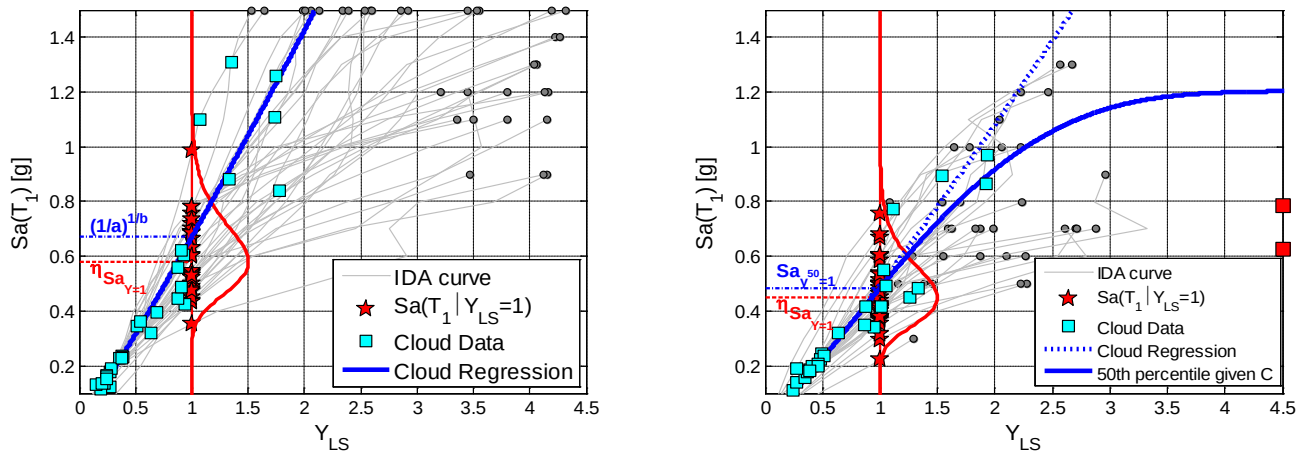

Fig. 7 – IDA curves, Cloud data, and the regression prediction for (a) Flexural Model, (b) Combined Model

According to Fig. 7a, for the Flexural model, $\eta_{SaY=1}$=0.58g while $\eta_{SaY=1,Cloud}=(1/a)^{1/b}$=0.67g. The difference between the results from Cloud analysis and IDA can be attributed to the fact that there are several Cloud data in the range of low *Sa* and low Y_{LS} values while the data around Y_{LS}=1 are not very well distributed. This seems to shift the Cloud prediction towards higher spectral acceleration values for Y_{LS}=1 which leads to over-estimation of the structural capacity. However, for the Combined Model in Fig. 7b, the blue-dotted line shows the Cloud regression on the *NoC* data while the blue-solid line reveals the 50th percentile y^{50}_{LS} (see Eq. 11). The value y^{50}_{LS} is the Cloud median prediction including the *C* data (shown by red squares). Although the regression prediction still seems to be governed by many Cloud data close to the origin, the Cloud analysis manage to adequately and more densely populate the zone of interest in the vicinity of Y_{LS}=1. As a result, the Cloud regression with y^{50}_{LS} lead to median spectral acceleration capacity estimate $\eta_{SaY=1,Cloud}$=0.48g which is very close to that obtained by the IDA with $\eta_{SaY=1}$=0.45g. Hence, it is quite important to ensure that the ground motion records selected for Cloud Analysis manage to properly distributed around Y_{LS}=1.

In order to have a better insight into the comparison between Cloud analysis and IDA results, Fig. 8 illustrates the 16th, 50th and 84th percentiles of performance variable Y_{LS} given *Sa* estimated based on both nonlinear dynamic procedures and for both Flexural and Combined Models. It can be seen that consideration of collapse information (as shown in Fig. 8b) properly manage to capture the trend in IDA results up to Y_{LS} around 1.5. Nevertheless, the results from both type of analyses deviates in case of Flexural model even for Y_{LS} values less than 1.

Finally, the resulting Log Normal fragility curves obtained based on IDA analysis for the above-mentioned two models are also potted as blue-dashed lines in Fig. 9. It can be observed that for the Flexural model (Fig. 9a), there is a decrease (shift) in the median of IDA fragility curve compared to the one from Cloud analysis (as revealed previously in Fig. 7a), while the dispersion of both fragilities are around 0.20. A better match between fragility curves is observed for the case of Combined Model in Fig. 9b, which can be contributed to the fact that Y_{LS} values are properly concentrated around the zone of interest (i.e., Y_{LS}=1) with respect to Flexural model. The dispersion of both fragility curves are estimated to be around 0.24 while there is a small decrease (shift) in the median associated with the IDA curve. This can also be appreciated by comparing the IDA and Cloud results shown in Fig. 7b.

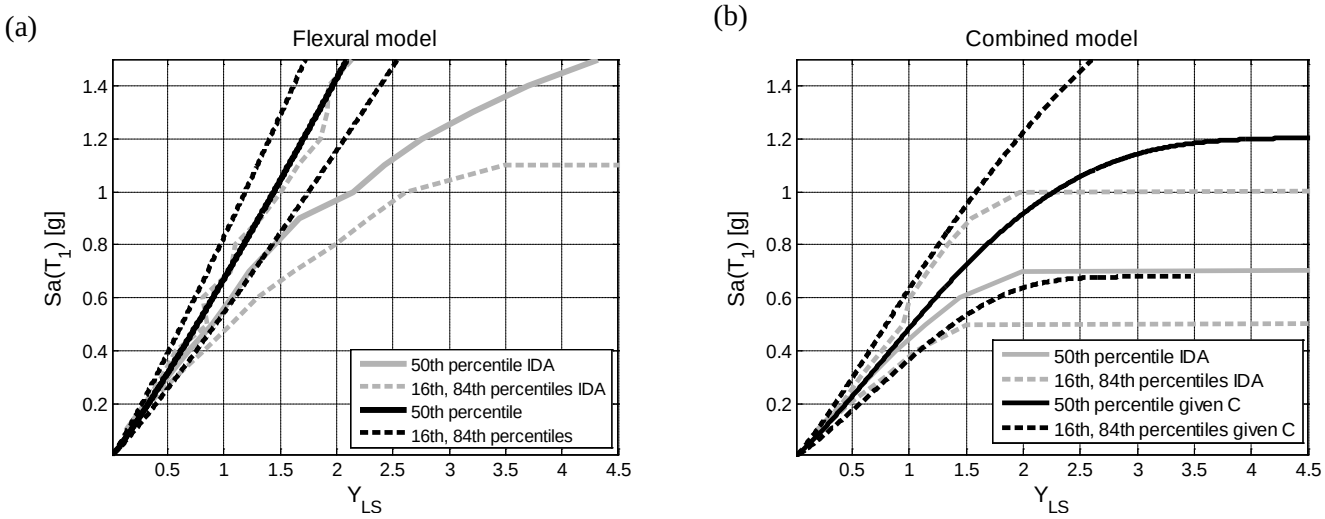

Fig. 8 – IDA vs. Cloud analysis, the 16th, 50th and 84th percentiles of performance variable Y_{LS} given *Sa* for (a) Flexural Model, (b) Combined Model

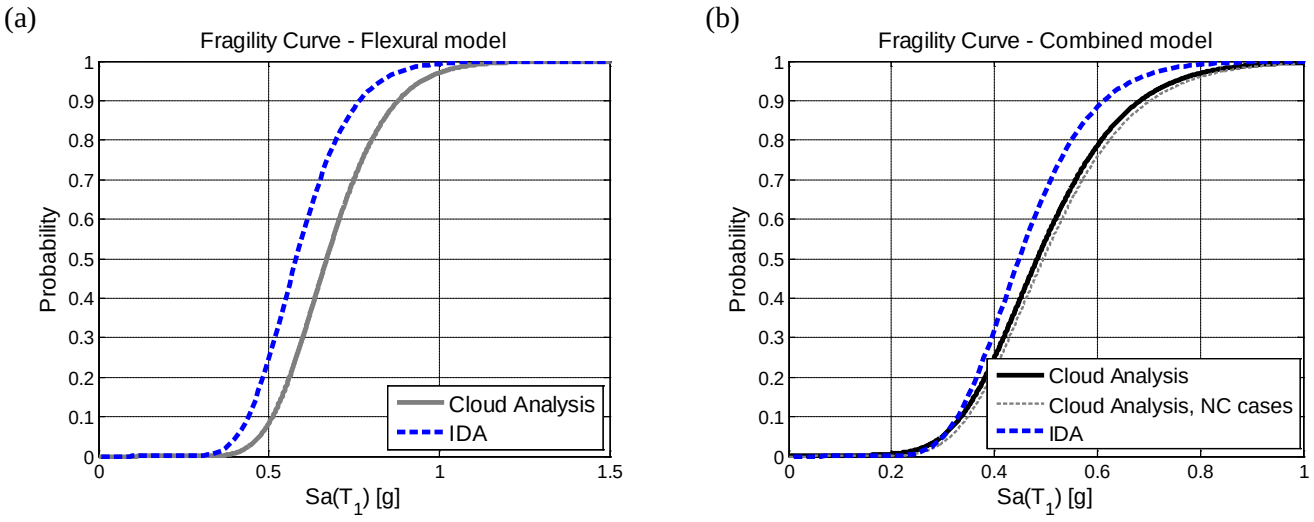

Fig. 9 – IDA vs. Cloud analysis, the fragility curves for (a) Flexural Model, (b) Combined Model

4. Conclusion

The Cloud Analysis is revisited here again by means of an efficient procedure which can account for cases when the structure becomes dynamically unstable; i.e. when the analysis software encounters non-convergence problems, or the Collapse of the building due to large demands takes place. The procedure allows for linear regression analysis on the "No-Collapse" data while a generalized linear regression model (Logistic regression herein) predicts the trend in "Collapse data". The procedure leads to development of fragility curves with the Collapse information explicitly included. In addition, the Cloud analysis procedure adopts for the global and systemic structural performance variable, denoted as Y_{LS}, defined as the demand over capacity ratio and calculated based on the reliability "cut-set" concept. Nevertheless, this performance variable is used not only for predicting the onset of limit state (when equals to unity), but also account for the possibility that some records may cause global Collapse of the building structure. Specifically, it is observed and concluded that:

- A systematic handling of the collapse cases is provided within the Cloud analysis procedure by mixing a simple logarithmic regression model and a logistic regression model.
- The proposed performance-based variable, Y_{LS}, defined based on cut-sets can overcome the need for identifying the Collapse cases by setting rather arbitrary thresholds.
- The Cloud analysis procedure with careful record selection can lead to reasonable results in comparison with IDA. This also helps in achieving the softening trend in the percentiles of EDP given IM within the Cloud analysis, which can be frequently seen through IDA.
- The records should be selected in a manner that the Cloud analysis manage to adequately and more densely populate the zone of interest in the vicinity of Y_{LS}=1. Note that pinning down the range of interest with Cloud data might not be achieved with the first round of structural analyses as it might require additional iterations involving scaling or modifications in the set of ground motion records.

5. Acknowledgements

This work is supported in part by the executive Project ReLUIS-DPC 2014/2016 (Work Package 3, Task5: Analysis of the seismic response of R.C. structural systems, and also Special Project RS11: The Uncertainties). This support is gratefully acknowledged.

6. References

[1] Cornell CA, Krawinkler H (2000): Progress and challenges in seismic performance assessment. *PEER Center News*, **3**(2), 1-3.

[2] Vamvatsikos D, Cornell CA (2004): Applied incremental dynamic analysis. *Earthquake Spectra*, **20**(2), 523-553.

[3] Jalayer F, Cornell CA (2009): Alternative non-linear demand estimation methods for probability-based seismic assessments. *Earthquake Engineering & Structural Dynamics*, **38**(8), 951-972.

[4] Bazzurro P, Cornell CA, Shome N, Carballo JE (1998): Three proposals for characterizing MDOF nonlinear seismic response. *Journal of Structural Engineering*, **124**(11), 1281-1289.

[5] Shome N, Cornell CA, Bazzurro P, Carballo JE (1998): Earthquakes, records, and nonlinear responses. *Earthquake Spectra*, **14**(3), 469-500.

[6] Cornell CA, Jalayer F, Hamburger RO, Foutch DA (2002): The probabilistic basis for the 2000 SAC/FEMA steel moment frame guidelines. *ASCE Journal of Structural Engineering*, **128**, 526–533, Special Issue: Steel Moment Resisting Frames after Northridge Part II.

[7] Jalayer F (2003): *Direct Probabilistic seismic analysis: implementing non-linear dynamic assessments*. Ph.D. dissertation, Stanford University, California.

[8] Jalayer F, Cornell CA (2003): A technical framework for probability-based demand and capacity factor design (DCFD) seismic formats. *Technical Report PEER 2003/08*, Pacific Earthquake Engineering Research, Berkeley, USA.

[9] Elefante L, Jalayer F, Iervolino I, Manfredi G. (2010) Disaggregation-based response weighting scheme for seismic risk assessment of structures. *Soil Dynamics and Earthquake Engineering*, **30**(2), 1513–1527.

[10] Jalayer F, De Risi R, Manfredi G (2015): Bayesian Cloud Analysis: efficient structural fragility assessment using linear regression. *Bulletin of Earthquake Engineering*, **13**(4), 1183-1203.

[11] Benjamin JR, Cornell CA (1970): *Probability, statistics and decision for civil engineers*. McGraw Hill, 684pp.

[12] Setzler EJ, Sezen H (2008): Model for the lateral behavior of reinforced concrete columns including shear deformations. *Earthquake Spectra*, **24**(2), 493-511.

[13] Sezen H (2008): Shear deformation model for reinforced concrete columns. *Structural Engineering and Mechanics* **28**(1), 39-52.

[14] Jalayer F, Franchin P, Pinto PE (2007): A scalar damage measure for seismic reliability analysis of RC frames. *Earthquake Engineering & Structural Dynamics*, **36**(13), 2059-2079.

[15] Ditlevsen O, Madsen HO (1996): *Structural reliability methods*, Wiley, New York.

[16] Galanis PH, Moehle JP (2015): Development of Collapse Indicators for Risk Assessment of Older-Type Reinforced Concrete Buildings. *Earthquake Spectra*, **31**(4), 1991-2006.

[17] Krawinkler H (2005): Van Nuys hotel building testbed report: exercising seismic performance assessment. *Technical Report PEER 2005/11*, Pacific Earthquake Engineering Research, Berkeley, USA.

[18] Scott MH, Fenves GL (2006): Plastic hinge integration methods for force-based beam–column elements. *Journal of Structural Engineering*, **132**(2), 244-252.

[19] Sezen H, Moehle JP (2004): Shear strength model for lightly reinforced concrete columns. *Journal of Structural Engineering*, **130**(11), 1692-1703.

[20] Gerin M, Adebar P (2004): Accounting for shear in seismic analysis of concrete structures. *13th World Conference on Earthquake Engineering*, Vancouver, B.C., Canada.

[21] Bentz EC (2000). *Sectional Analysis of Reinforced Concrete Members*. PhD dissertation, Department of Civil Engineering, University of Toronto, 2000, 310 pp.

[22] Elwood KJ, Moehle, JP (2005): Axial capacity model for shear-damaged columns. *ACI Structural Journal* **102**, 578-587.

[23] Silva WJ (1998): Pacific Engineering and Analysis Strong-Motion Catalog, *Pacific Engineering and Analysis*, Pacific Engineering & Analysis, 311 Pomona Ave. El Cerrito, CA 94530, http://peer.berkeley.edu/smcat/ .